(54) Titre : SYSTEME ET METHODE DE MESURE DU SIGNAL DPOAE
(54) Title: DPOAE MEASUREMENT SYSTEM AND METHOD

(57) Abrégé/Abstract:

A new method of DPOAE signal level measurement based on a recently developed family of nonlinear adaptive algorithms is presented. Three core units are employed to extract and measure the two artifacts and the DPOAE signal. Each core unit, which can be any of the three members of a new family of signal processing algorithms, has the capability to lock on and track the time variations of a specified sinusoidal component of its input signal. The core units have very simple structure while maintaining very good performance in noisy environments in terms of stability and convergence speed. Performance of the present method is demonstrated with the aid of computer simulations. The present method features structural simplicity which renders it suitable for both software and hardware implementation. It offers extremely high noise immunity and requires shorter measurement time than conventional methods.

DPOAE MEASUREMENT SYSTEM AND METHOD

Abstract

A new method of DPOAE signal level measurement based on a recently developed family of nonlinear adaptive algorithms is presented. Three core units are employed to extract and measure the two artifacts and the DPOAE signal. Each core unit, which can be any of the three members of a new family of signal processing algorithms, has the capability to lock on and track the time variations of a specified sinusoidal component of its input signal. The core units have very simple structure while maintaining very good performance in noisy environments in terms of stability and convergence speed. Performance of the present method is demonstrated with the aid of computer simulations. The present method features structural simplicity which renders it suitable for both software and hardware implementation. It offers extremely high noise immunity and requires shorter measurement time than conventional methods.

1

Introduction

Distortion product otoacoustic emissions (DPOAEs) are very low level stimulated acoustic responses to two pure tones presented to the ear canal. DPOAE measurement provides an objective non-invasive measure of peripheral auditory function and is used for hearing assessment [1]. DPOAE screening is becoming a standard clinical practice to predict potential sensorineural hearing loss especially in newborns.

DPOAEs have been recognized for a number years [2, 3]. However, DPOAE measurement is considered an active area of research because of the challenging nature of the signal processing task. To address the ever-increasing demand for high performance DPOAE measurement methods, a number of signal processing algorithms have been present in recent years [1, 4-6]. With the availability of the powerful computational tools such as digital signal processors (DSPs), commercial medical equipment dedicated to DPOAE measurement are becoming available [7-14].

In this type of otoacoustic test, two pure tones with frequencies f_1 and f_2 are presented to the cochlea. For best results, f_2 is usually chosen as $1.2f_1$. Due to the non-linearity of ear, a very low level of distortion product of frequency $2f_1 - f_2$ is generated in normal ears. The level of such DPOAE signal is a measure of functionality of the ear. Estimation of such a weak signal buried under two strong artifacts in a potentially noisy background is a challenging signal processing problem.

Conventionally, fast Fourier transform (FFT) is used as the main signal processing tool to estimate the level of DPOAE signals. Application of FFT in this problem has a number of shortcomings among which long measurement time is most pronounced. Such long measurement time is usually required for acquisition of more data which, when averaged, reduce the overall background noise effect. Unreliability of the measurements is another

2

problem of FFT-based methods and is a direct effect of the sensitivity of the FFT-based methods to the background noise. In addition to the need to increase the measurement time, the tests are usually required to be conducted in low noise environments such as sound-proof booths.

In attempt to devise high performance DPOAE estimation techniques, linear adaptive signal processing techniques have been employed [1, 4, 14]. Such techniques generally offer better performance in terms of measurement time which may be interpreted as higher noise immunity of adaptive techniques compared to FFT. However, the need for sound-proof examination rooms is not obviated with such techniques.

This document presents a method of measurement of DPOAE signals based on a new signal processing technique in which individual sinusoidal components of a given signal are extracted and their variations are adaptively tracked over time. The core units are presented in a separate disclosure [15]. The present DPOAE estimation method consists of three units which can be any of the three such algorithms. The two artifacts are first extracted by two units and are subtracted from the input signal to generate an input signal of which DPOAE signal has a higher relative portion. Such a signal is then fed to another core unit which estimates the level of DPOAE signal. Superior performance of the present technique in terms of noise immunity and fast measurements is illustrated with the aid of computer simulations.

In order to provide a brief background on the subject, a general review of the structure of a generic DPOAE measurement device is presented in the next section. It will be seen that the heart of such an apparatus is the signal processing subsystem which, in the final analysis, determines the performance of the overall system. Section presents the present scheme for such signal processing module. The core units which are the building blocks of the present signal processing scheme are introduced in section . Performance of the

3

present method is demonstrated in section .

Structure of a Generic DPOAE Measurement Device

In this section a brief overview of the structure of a typical DPOAE detection system is provided. Figure 1 shows the generic block diagram of a DPOAE measurement device. It consists of three main modules: the data acquisition/transducers module, the signal processing module and the display.

Data acquisition unit is the medium between the processing unit and the probe which transmits and receives acoustic signals in the audio range. Components of the compound data acquisition/transducers module are illustrated in more detail in Figure 2. One of the main functions of this module is to convert digital signals produced by the signal processing module to analog signals which are then conditioned and converted to audio signals. Conditioning of the signals in this case may or may not include filtering. Conversely, the audio signals recorded by the probe are conditioned and converted to digital signals to be processed by the signal processing module.

The signal processing module is the heart of the system which produces the digital form of the artifacts and extracts and measures the DPOAE signal. A DSP, or if the computational/architectural demand is low even a microcontroller, can be employed as the hardware platform of this unit. Signal processing is embedded as the software in such a hardware platform. Alternatively, and provided that the complexity of the signal processing algorithms remains low, signal processing unit may be implemented solely in hardware using programmable logic array (PLA) or field programmable gate array (FPGA) technology. In an ideal case, namely when the signal processing algorithm is not excessively complex, the hardware does not require a PC for its operation; however, interfacing to a

4

PC is usually provisioned for data management.

The display unit is the interface between the device and the operator. It can be a simple LED/LCD and/or a small printer.

Present Technique

Figure 3 shows the main functions of the software embedded in the signal processing module. The software is essentially responsible for the generation of the artifact signals and extraction of DPOAE as well as management of input/output data. As discussed before, the significance of the present work is in the introduction of a signal processing technique for the extraction and measurement of DPOAE signals.

The present signal processing scheme employs three core units to construct a high performance DPOAE extraction module. The three possible structures of such building block units are presented in section . Each core unit is capable of focusing on and extracting a pre-specified sinusoidal component of its input signal which may contain many other components including noise. More importantly, they can effectively follow variations in the amplitude, phase (and frequency) of the extracted sinusoidal component. Although the underlying mathematics ensuring stability and performance of such core units is very complex, the structure of the core units remain extremely simple. They are found to be very robust with respect to variations in the internal settings as well as external conditions and exhibit superior performance over existing linear adaptive and FFT-based algorithms.

The input signal is often assumed to consist of two pure sinusoids with frequencies f_1 and f_2 at a very high level (usually about $60 - 70$ dB) and a very low level DPOAE $2f_1 - f_2$ at about 0 dB. It is polluted by a noise usually considered to be at about -10 dB level. The

5

noise in fact represents the totality of all undesirable signals that may be present in the environment in which the examination is being conducted as well as unavoidable white Gaussian noise. Because of excessive degree of pollution (artifacts and noise), one single core unit set to extract the DPOAE signal out of the input exhibits poor performance. Different arrangements were studied to construct a high performance architecture. The most successful configuration is shown in Figure 4. Three core units are employed. The first two core units are set to extract the artifacts. They effectively do so with very small errors. The extracted artifacts are then subtracted from the input to produce a signal, of which DPOAE has a higher relative portion. The third core unit is then set to extract DPOAE.

Review of the Core Unit

This section reviews the mathematical structure and properties of the core units which are the basis for the present DPOAE measurement method of section . A complete description of the signal processing core is provided in [15]. Let $u(t)$ denote a signal comprising a number of individual sinusoidal components and noise, expressed by

$$u(t) = \sum_{k=1}^{N} A_k \sin \phi_k + n(t) \tag{1}$$

where $\phi_k = \omega_k t + \theta_k$ is the total phase, and $n(t)$ denotes the total noise imposed on the signal. The objective is to find a scheme for estimating a certain component of such input signal as fast and accurate as possible; a scheme which should not be sensitive to the noise and the potential time variations of the input signal. Simplicity of the structure, for the sake of practical feasibility, is desirable.

Let $\mathcal{M}$ be a manifold containing all pure sinusoidal signals defined as

$$\mathcal{M} = \{y(t,\theta) = \theta_1 \sin(\theta_2 t + \theta_3) | \ \theta_i \in [\theta_{i,\min}, \theta_{i,\max}]\}$$

6

where $\theta = [\theta_1, \theta_2, \theta_3]^T$ is the vector of parameters which belongs to the parameters space

$$\Theta = \{[\theta_1, \theta_2, \theta_3]^T \mid \theta_i \in [\theta_{i,\min}, \theta_{i,\max}]\}$$

and T denotes matrix transposition. To extract a certain sinusoidal component of $u(t)$, the solution has to be an orthogonal projection of $u(t)$ onto the manifold $\mathcal{M}$, or equivalently has to be an optimum θ which minimizes a distance function d between $y(t, \theta)$ and $u(t)$, i.e.,

$$\theta_{\text{opt}} = \arg\min_{\theta \in \Theta} d(y(t, \theta), u(t)).$$

In least squares method, d is the instantaneous distance function

$$d^2(t, \theta) = (u(t) - y(t, \theta))^2 \triangleq e(t)^2.$$

The parameter vector θ is estimated using the gradient descent method,

$$\frac{d}{dt}\theta(t) = -\mu \frac{\partial}{\partial \theta}(d^2(t, \theta))$$

where the positive diagonal matrix μ is the algorithm regulating constant. It controls the convergence rate as well as the stability of the algorithm.

Following the steps outlined above, three possible sets of differential equations are obtained depending on the definition of the form of the parameter θ. Complete derivations are presented in [15]. The governing sets of equations of all three members of this family of the algorithms can be written under the same formulation as

$$\dot{A} = \mu_1 e \sin\phi, \tag{2}$$

$$\dot{\omega} = \mu_2 e A \cos\phi, \tag{3}$$

$$\dot{\phi} = F(A, \omega, \phi, e), \tag{4}$$

$$y(t) = A \sin\phi, \tag{5}$$

$$e(t) = u(t) - y(t), \tag{6}$$

where $y(t)$ is the output and the function $F(A, \omega, \phi, e)$ can take any of the following forms:

7

- Type 1: $F(A, \omega, \phi, e) = \mu_2 e A \cos\phi + \omega_o,$

- Type 2: $F(A, \omega, \phi, e) = \omega,$

- Type 3: $F(A, \omega, \phi, e) = \mu_3 e A \cos\phi + \omega$

where ω_o is a fixed center frequency. The dynamics resulting from the first of these forms can be expressed in a more concise way as

$$
\begin{aligned}
\dot{A} &= \mu_1 e \sin\phi, \\
\dot{\phi} &= \mu_2 e A \cos\phi + \omega_o, \\
y(t) &= A \sin\phi, \\
e(t) &= u(t) - y(t).
\end{aligned}
$$

It has been shown that each of the three dynamical systems represented by the above sets of differential equations possesses a unique asymptotically stable periodic orbit which lies in a neighborhood of the orbit associated with the desired component of the function $u(t)$. In terms of the engineering performance of the system, this indicates that the output of the system $y(t) = A \sin\phi$ will approach a sinusoidal component of the input signal $u(t)$. Moreover, the slow variations of parameters in $u(t)$ are tolerated by the system.

Figure 5 shows implementation of the algorithms in the form of composition of simple blocks suitable for schematic software development tools. Numerically, a possible way of writing the set of equations governing the present algorithm in discrete form, which can be readily used in any programming language, is

$$
\begin{aligned}
A[n+1] &= A[n] + T_s \mu_1 e[n] \sin\phi[n], \\
\omega[n+1] &= \omega[n] + T_s \mu_2 e[n] A[n] \cos\phi[n], \\
\phi[n+1] &= \phi[n] + T_s F(A[n], \omega[n], \phi[n], e[n]),
\end{aligned}
$$

8

$$y[n] = A[n]\sin\phi[n],$$
$$e[n] = u[n] - y[n]$$

where a first order approximation for derivatives is assumed, T_s is the sampling time and n is the index of iteration.

The dynamics of each of the three algorithms presents a notch filter in the sense that it extracts (i.e. lets pass through) one specific sinusoidal component and rejects all other components including noise. It is adaptive in the sense that the notch filter accommodates variations of the characteristics of the desired output over time. The center frequency of such adaptive notch filter is specified by the value of ω_o in the first type or the initial condition of the variable ω in the second and third type.

A physical system approaches its steady state in about a few times its time constant $\tau = \frac{1}{\mu}$ where μ represents the eigenvalue of the system. The eigenvalues of the presented dynamical systems are $-\frac{\mu_1}{2}$ and $-\frac{\mu_2}{2}A^2$, which determine the speed of the system in approaching the solution. For example, a set of values of $\mu_1 = \mu_2 = 10000$ should cause the introduced dynamical systems to reach their steady state in about $5\tau = 1$ ms for an input signal of unit amplitude.

It has been observed that all three types of the algorithms introduced in this section can be employed as the core units of the present DPOAE measurement scheme of Figure 4. For the purpose of demonstration of the performance of the algorithms and the DPOAE measurement scheme, type 1 algorithm is used throughout this document as the building block. Figure 6 shows the performance of one such unit in the extraction of a specified sinusoidal component of its input signal. As noted before, the specification of the desired sinusoidal component is achieved by means of appropriate setting of parameter $\omega_o = 2\pi f_o$ which determines the frequency of the component of interest. The input signal is a clean sinusoid of frequency $f = 3000$ Hz with a random constant phase. All the initial conditions

9

are taken as zero. As would be expected, the convergence is achieved within about 1 ms.

When the input signal consists of a single pure sinusoid which is to be extracted, the values of the parameters μ_1 and μ_2 can be chosen very large so as to increase the speed of convergence without any trade-off with accuracy. However, as the degree of the pollution in the input signal, which may be quantitatively represented by total harmonic distortion (THD) or signal to noise ratio (SNR) increases, there will always be a trade-off between the speed and accuracy. Figure 7 shows the performance of the single unit set as before for a sinusoidal input polluted by a white Gaussian noise with SNR=20 dB. With this parameter setting, a noise of 100% magnitude in the input introduces about 5% error in the estimated value of the amplitude. The same experiment is now repeated with a much smaller values of parameters μ_1 and μ_2. Figure 8 shows the result of this case. It is clear that a reduction of parameters by a factor of 60 results in a convergence time of about 60 times longer. For this, one gains a reduction in the incurred error of a factor of about 10.

Another factor to be considered in the assignment of values to parameters μ_1 and μ_2 is the amplitude of the input signal. As noted before, the eigenvalues of the algorithm are $-\frac{\mu_1}{2}$ and $-\frac{\mu_2}{2}A^2$. The first one is merrily independent of the input signal, but the second one is dependant on the amplitude of the input signal. In order to achieve the same speed of convergence when the amplitude of the input signal is reduced, one has to increase the value of the parameter μ_2 by the square of the reduction factor. Figure 9 shows the performance of the algorithm when this provision is made which verifies the theoretical prediction.

10

Performance

This section presents the performance of the present technique by the use of computer simulations. Three core units of the first type are used in the arrangement of Figure 4 to construct the present DPOAE measurement scheme. All the initial conditions are taken to be zero. The first two units which are employed to extract the artifacts must do so with as small an error as possible to produce an input to the third unit containing DPOAE signal as a main component, otherwise the third unit will not be able to extract DPOAE signal with sufficient accuracy. Therefore, the parameters are chosen relatively small at $\mu_1 = 100$ and $\mu_2 = 50$. With these values, it is expected that the convergence is achieved within about 100 ms. The same setting was also found suitable for the third unit. Two forces oppose each other in the selection criteria for the values of the parameters of the third unit. On the one hand, since SNR is very low for the third unit (DPOAE being taken as the signal and the total residual errors of the first two units as the noise), the parameters must be very small. On the other hand, since the input has a very low level, the value of μ_2 must be large. These two forces seem to cancel each other for the case of μ_2 so that the original value of 50 remains a good choice. As for the value of μ_1, one expects that it should be small to achieve acceptable accuracy in the extracted signal. This is true, but since only the amplitude of the extracted signal (i.e. the level of DPOAE) is of interest, one can substantially increase μ_1. The accuracy in the estimated extracted signal (and not necessarily its amplitude) is thus traded off which in this case is not of importance. The estimation of the amplitude remains accurate while the convergence speed is high enough. At any rate, a rough setting of the values of parameters μ_1 and μ_2 are to be done. The core algorithms have been shown to be very insensitive with regard to the settings of the parameters; variations as much as 50% in the values of these parameters seem to have practically no effect on the performance. The value of the amplitude directly estimated by the third unit was used as the estimate of the level of DPOAE.

11

The input signal is synthesized by the summation of two artifacts at frequencies $f_1 = 3000$ Hz and $f_2 = 1.2f_1 = 3600$ Hz and the DPOAE signal at $2f_1 - f_2 = 2400$ Hz. The amplitude of the artifacts are taken as 1 v and the DPOAE level is 0.5 mv. With these values, the level of the artifacts is set at about 66 dB higher than that of DPOAE. Figure 10 shows the performance of the present technique. It is confirmed that the measurement is completed in about 100 ms.

To present the dynamic performance of the present algorithm, the response of the algorithm to a step change in the level of DPOAE signal is presented in Figure 11. It is clear that the algorithm follows the variations in the level of DPOAE at a sufficiently high speed.

A number of measurements can be made consecutively. Figure 12 shows such an example. In each case, the frequency of the extracted DPOAE signal is shown. As the frequency decreases, less number of cycles are available in a given time interval. For example, there are 160 cycles available in 100 ms of a signal of frequency $f = 1600$ Hz whereas in the case of a signal of frequency $f = 4000$ Hz the available number of cycles are 400 in the same time interval. This explains why the estimation of DPOAE level is better achieved at higher frequencies. It should be noted that within the range of frequencies of interest for DPOAEs, the algorithm provides acceptable estimates in about $100 - 200$ ms.

As noted before, one of the main features of the employed core algorithms is their noise immunity. Therefore, one expects that the overall DPOAE estimation scheme be immune to background noise. Usually, otoacoustic tests are conducted in quiet examination rooms so that the level of noise floor is low enough for good results. Under such controlled conditions, a noise floor of about 10 dB lower than DPOAE signal (SNR=10 dB) exists. It is obvious that an algorithm which is able to extract a DPOAE signal highly immersed in background noise is desirable in that it alleviates the need for special quiet examination

12

facilities such as sound-proof booths. Figure 13 shows the performance of the present algorithm in a highly noisy environment where the level of the DPOAE signal is set to be at the level of the noise floor (SNR=0 dB). The incurred error is negligible. In Figure 14, the level of noise is elevated to be 10 times larger than the that of DPOAE signal itself. The incurred estimation error is less than $\pm15\%$ which for most practical application is sufficiently good. The excellent noise immunity of the present algorithm not only obviates the need for sound-proof examination rooms, but also provides the way to reduce the level of the artifacts for more patient-friendly tests.

References

[1] Ö. Özdamar and R. E. Delgado, "Otoacoustic emission acquisition using adaptive noise cancellation techniques," 2nd *International Biomedical Engineering Days,* IEEE 1997, pp. 139-143.

[2] D. T. Kemp, "Stimulated acoustic emissions from within the human auditory system," *J. Acoust. Soc. Am.,* Vol. 64, No. 5, 1978, pp. 1386-1391.

[3] R. Probst, B. L. Lonsbury-Martin, and G. K. Martin, "A review of otoacoustic emissions," *J. Acoust. Soc. Am.,* Vol. 89, No. 5, 1991, pp. 2027-2067.

[4] W. K. Ma and Y. T. Zhang, "Estimation of distortion product otoacoustic emissions," *IEEE Transactions on Biomedical Engineering,* Vol. 46, No. 10, October 1999, pp. 1261-1264.

[5] M. Du, F. H. Y. Chan, F. K. Lam, J. Ren, "Design consideration of a multi-function otoacoustic emission measurement system," *Proceedings of the 20th Annual International Conference of the IEEE Engineering in Medicine and Biology Society,* Vol. 20, No. 4, 1998, pp. 1928-1931.

[6] R. S. Kulik, H. Kunov, "Results of two types of averaging for distortion product otoacoustic emission measurement," *Proceedings of 1995 IEEE-EMBC and CMBEC,* pp. 979-980.

[7] Otodynamics Ltd., http://www.otodynamics.com

[8] Grason-Stadler Inc., 1 Westchester Drive, Milford, NH 03055, USA

[9] Etymōtic Research, http://www.etymotic.com

[10] Starkey Laboratories Inc., http://dp2000.starkey.com /dp2000/public-clear

[11] Madsen Electronics, http://www.madsen.com

[12] Bio-logic Systems Corp., http://www.blsc.com/products/audx/

[13] Intelligent Hearing Systems, http://www.gate.net/ ihs1

[14] Vivosonic Corp., http://www.vivosonic.com

[15] A. K. Ziarani, "System and method of extraction of sinusoids of time-varying characteristics," *Canadian Patent Pending.*
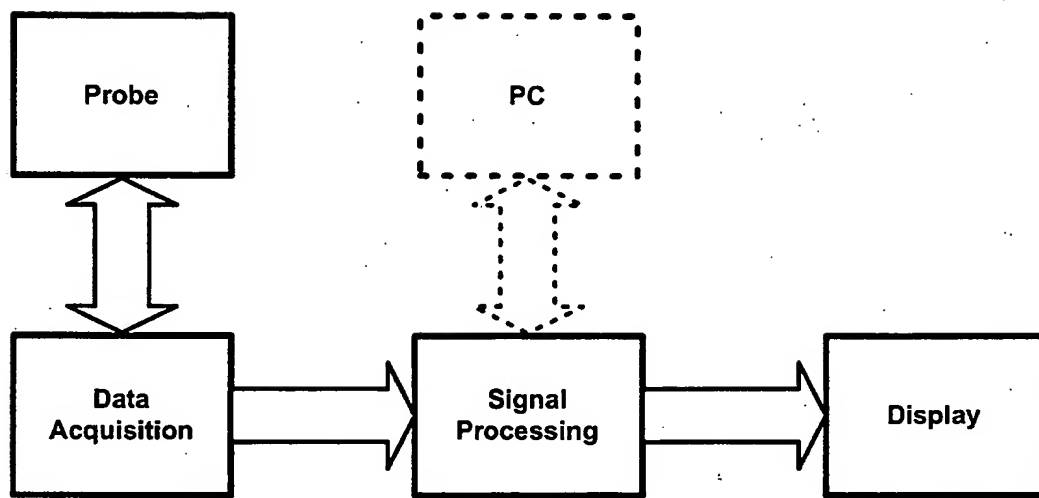
Figure 1: Generic block diagram of a DPOAE measurement device.
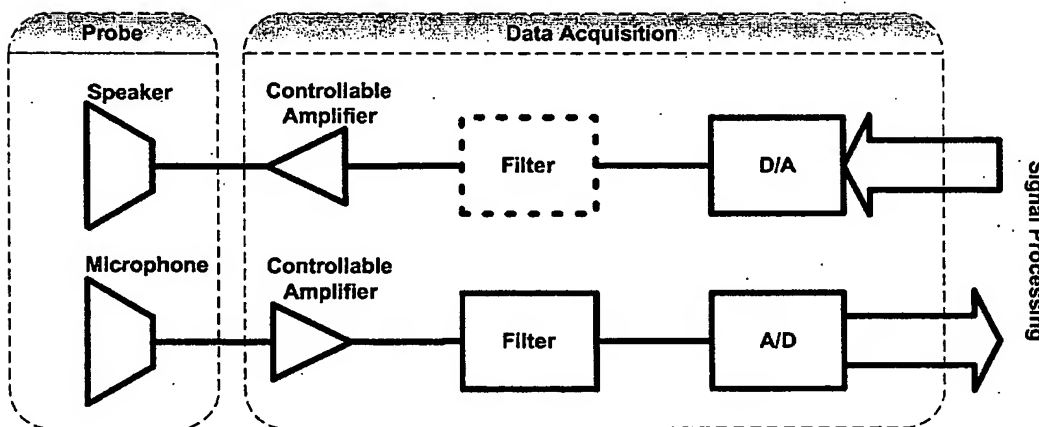
Figure 2: A more detailed diagram of data acquisition and probe units.

1
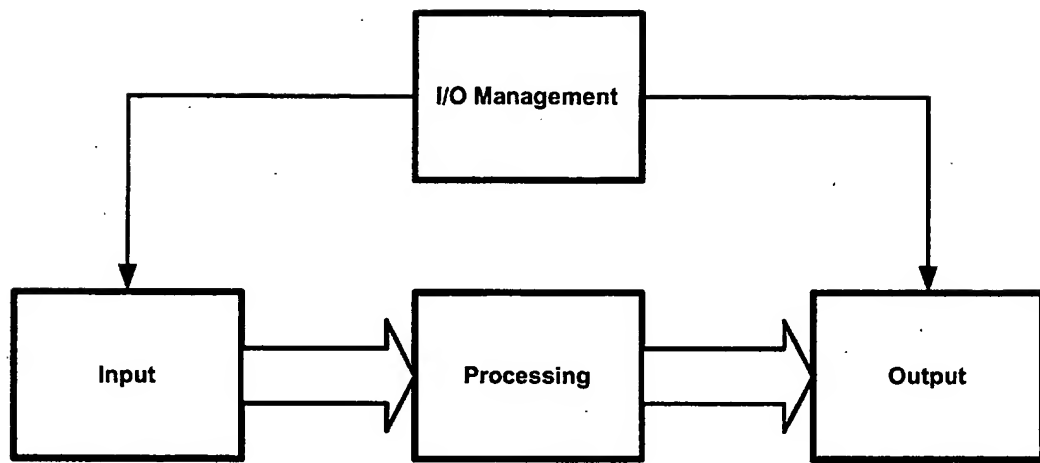
Figure 3: Main functions of the embedded software.
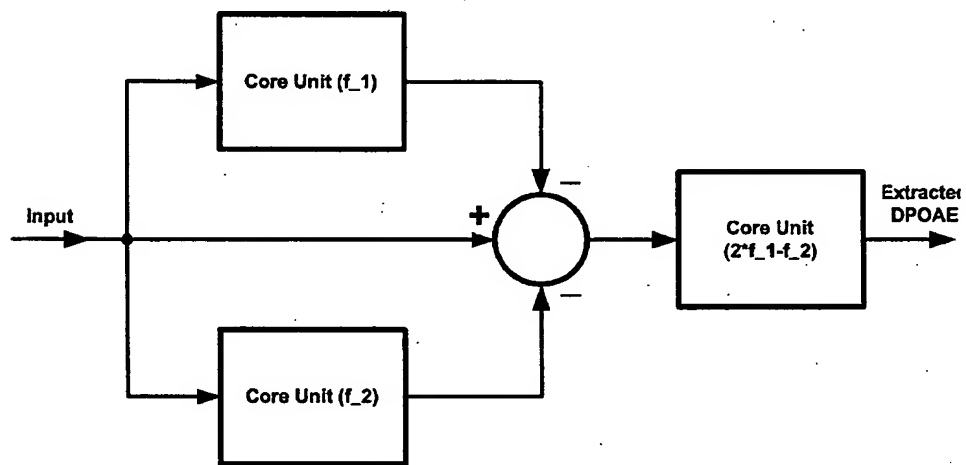
Figure 4: Block diagram of the signal processing scheme.

2
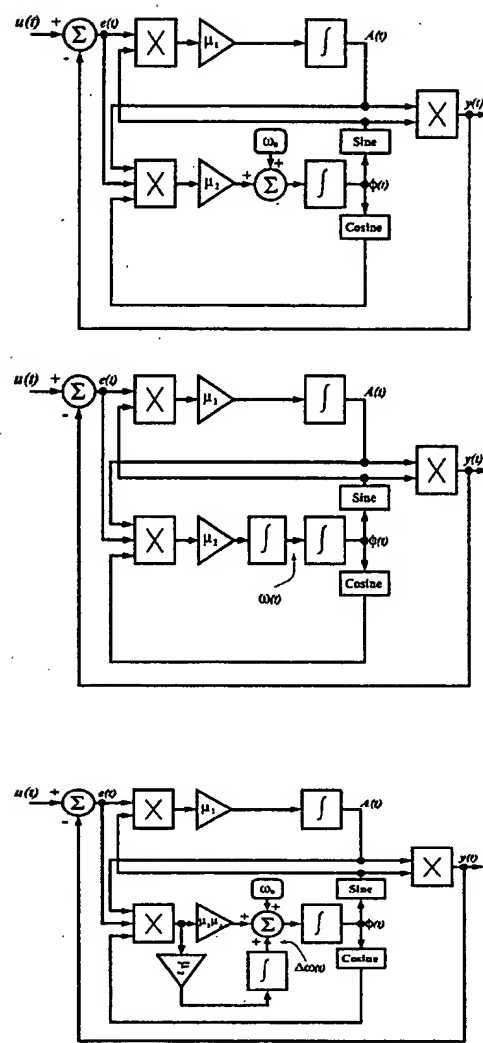
Figure 5: Block diagram implementation of the three possible core units of type $1 - 3$.

3
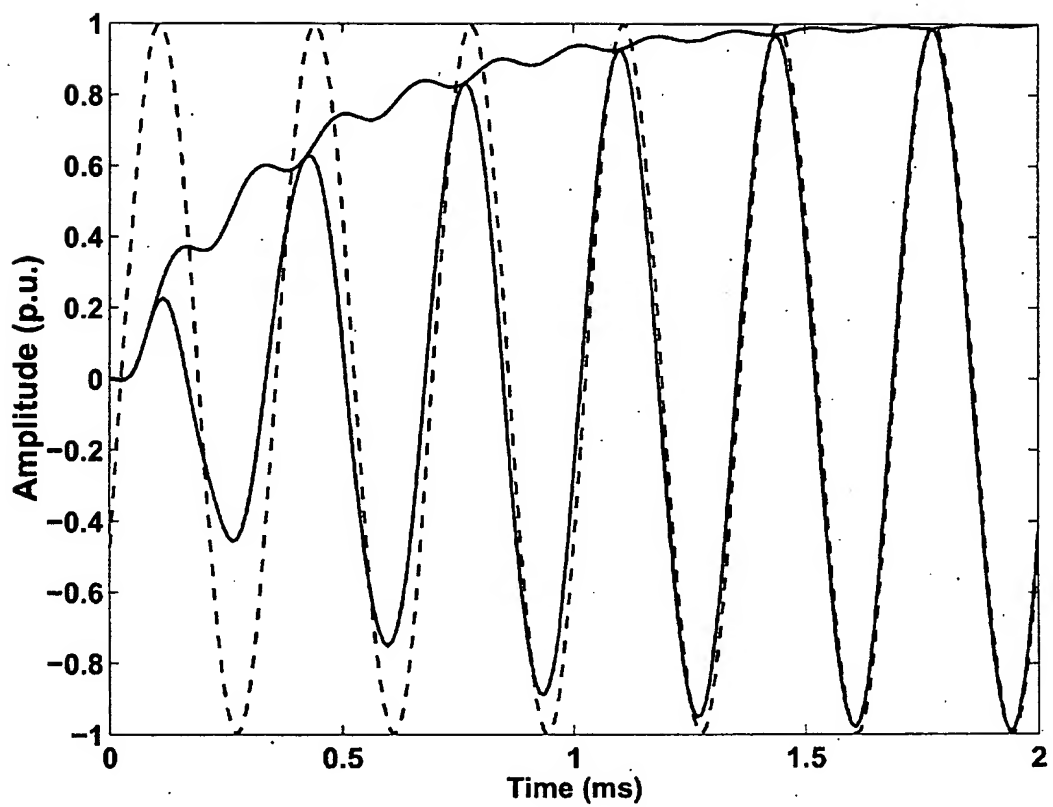
Figure 6: Performance of a single unit in the extraction of a sinusoidal component and its amplitude. The dashed line waveform is the input. The parameters are set at $\mu_1 = 12000$ and $\mu_2 = 6000$.

4
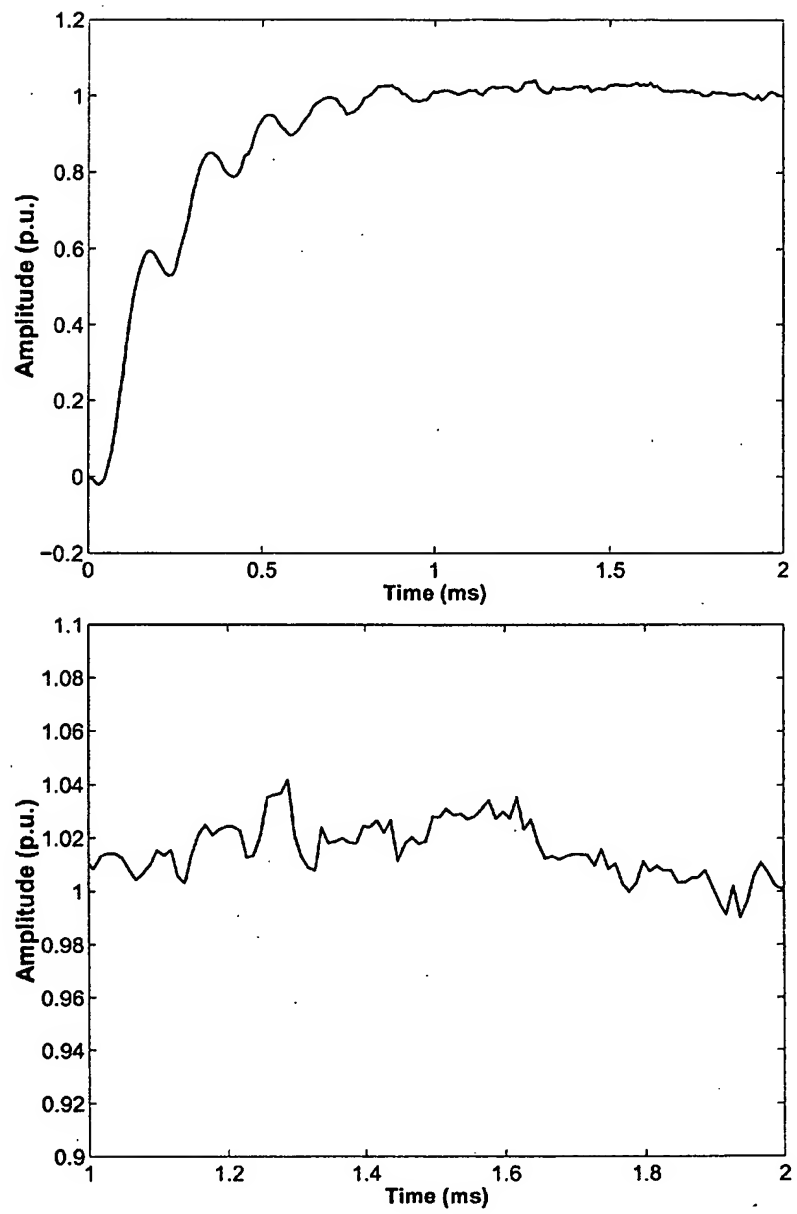
Figure 7: Performance in the presence of noise. The parameters are set at $\mu_1 = 12000$ and $\mu_2 = 6000$. The bottom figure is a magnified portion of the top figure.

5
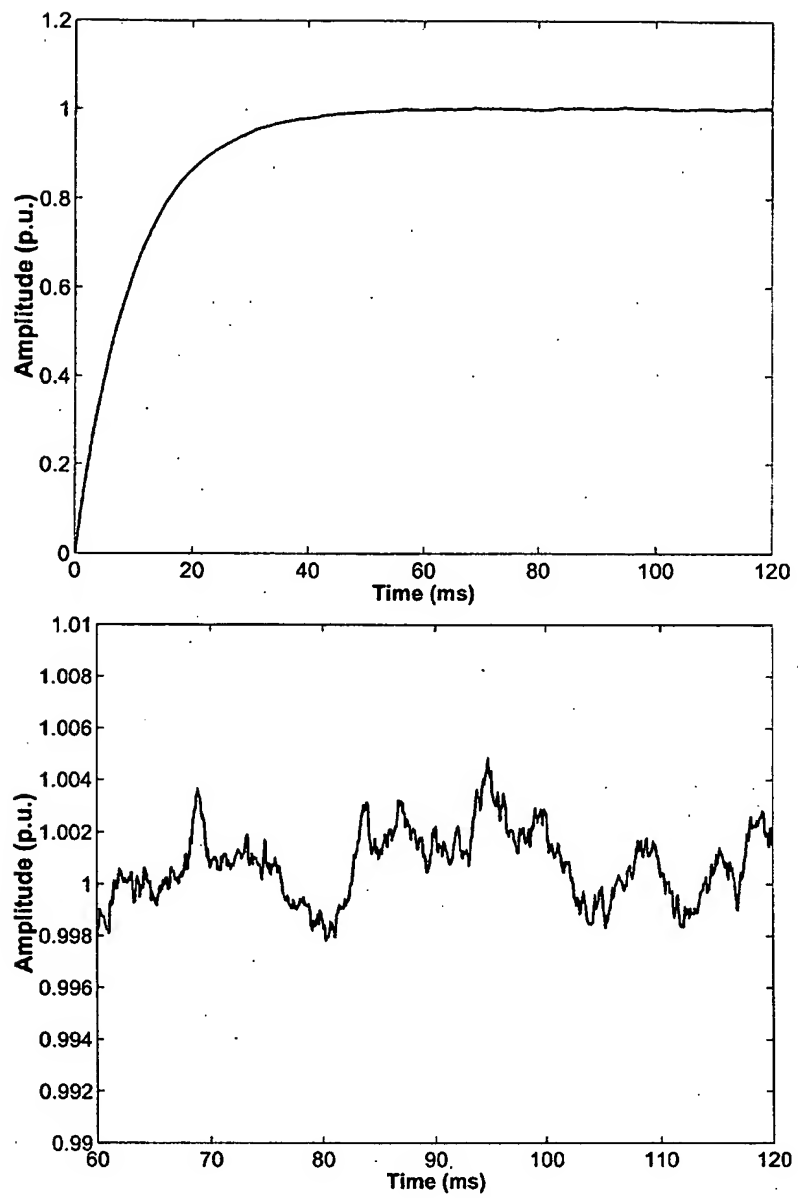
Figure 8: Performance in the presence of noise. The parameters are set at $\mu_1 = 200$ and $\mu_2 = 100$. The bottom figure is a magnified portion of the top figure.

6
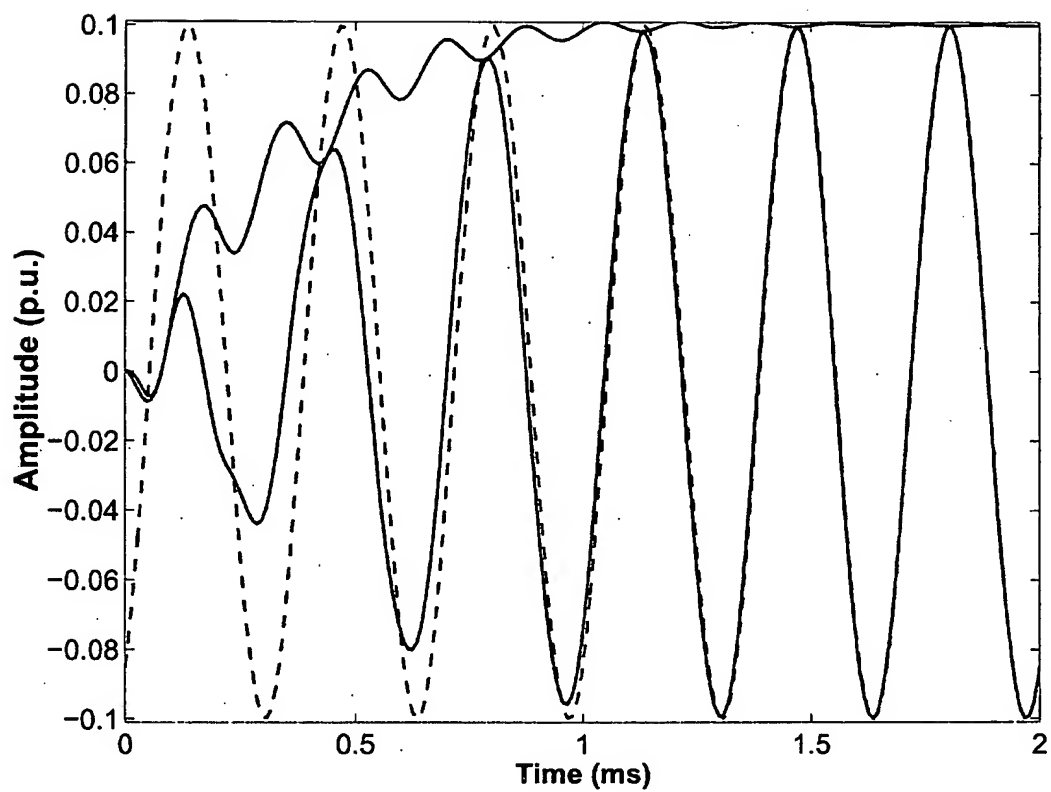
Figure 9: Performance of a single unit in the extraction of a sinusoidal component and its amplitude when the amplitude of the input signal is reduced by factor of 10. The dashed line waveform is the input. The parameters are set at $\mu_1 = 12000$ and $\mu_2 = 6000 \times (10)^2$.

7
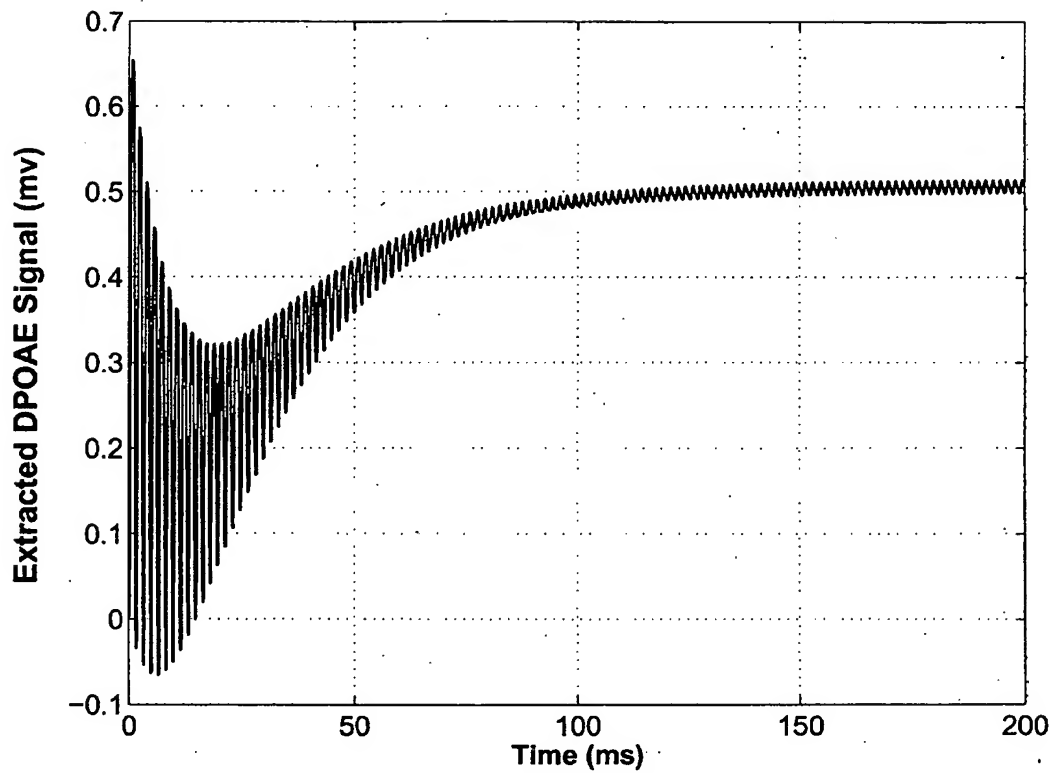
Figure 10: Performance of the DPOAE estimation method in measurement of a signal of 0.5 mv amplitude.
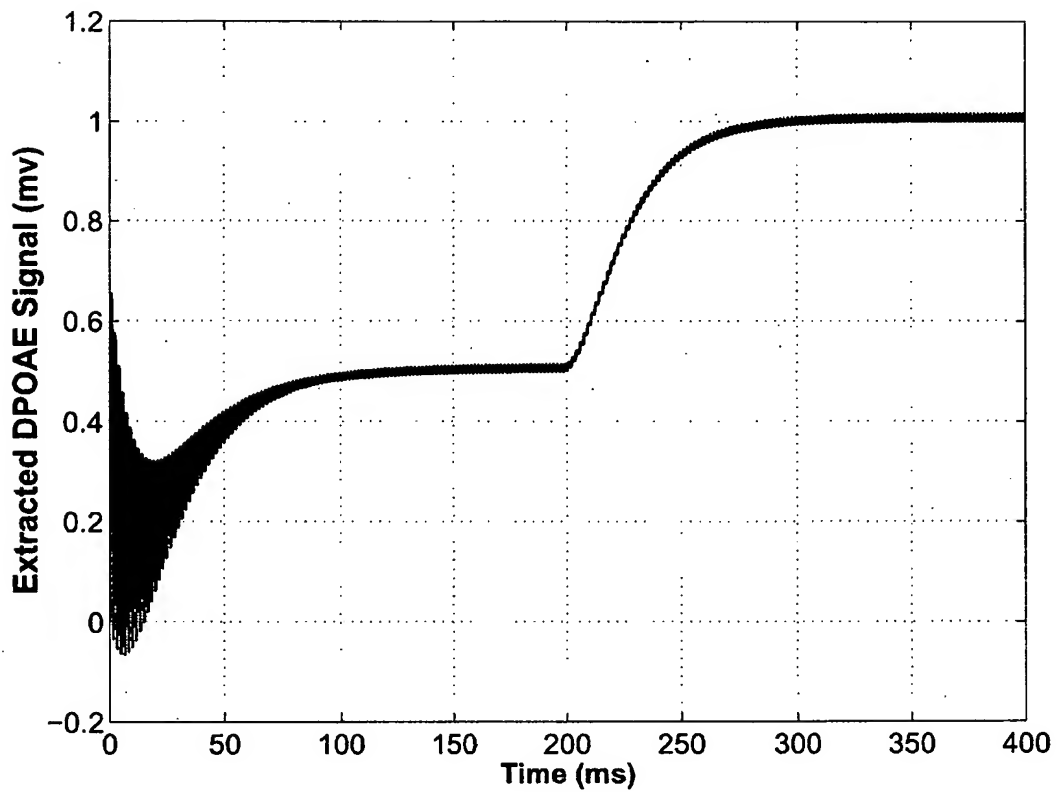
Figure 11: Dynamic performance of the present method. The level of DPOAE undergoes a step change at $t = 200$ ms.

9
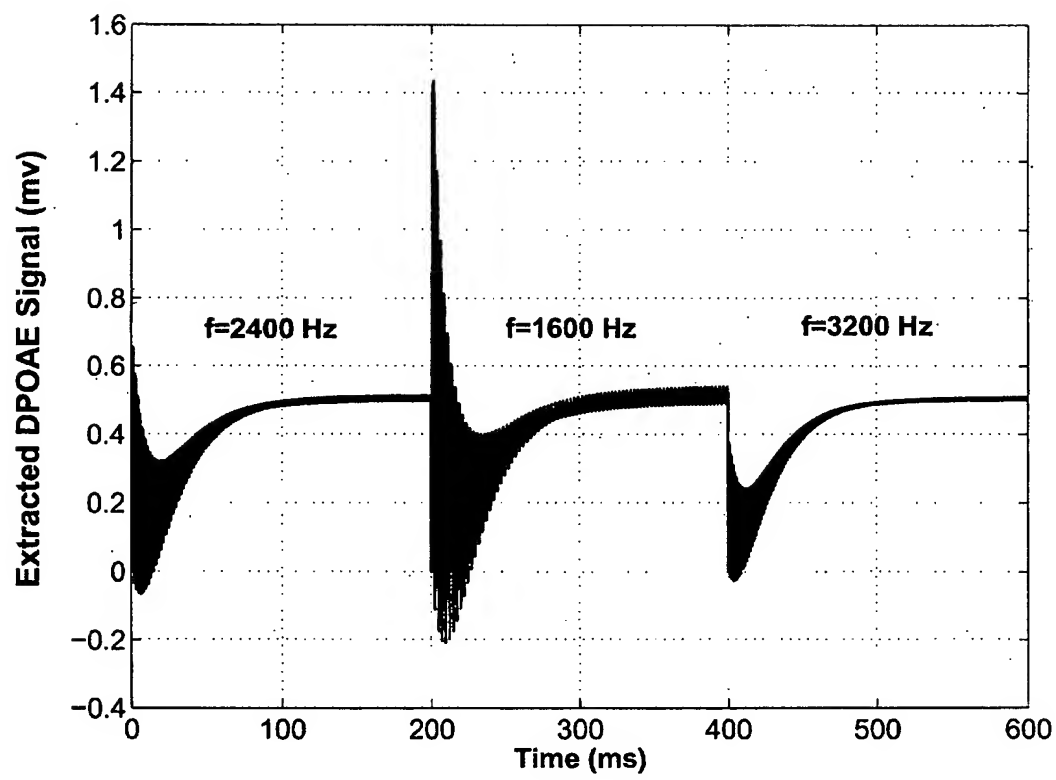
Figure 12: Three consecutive measurements with different frequencies.

10
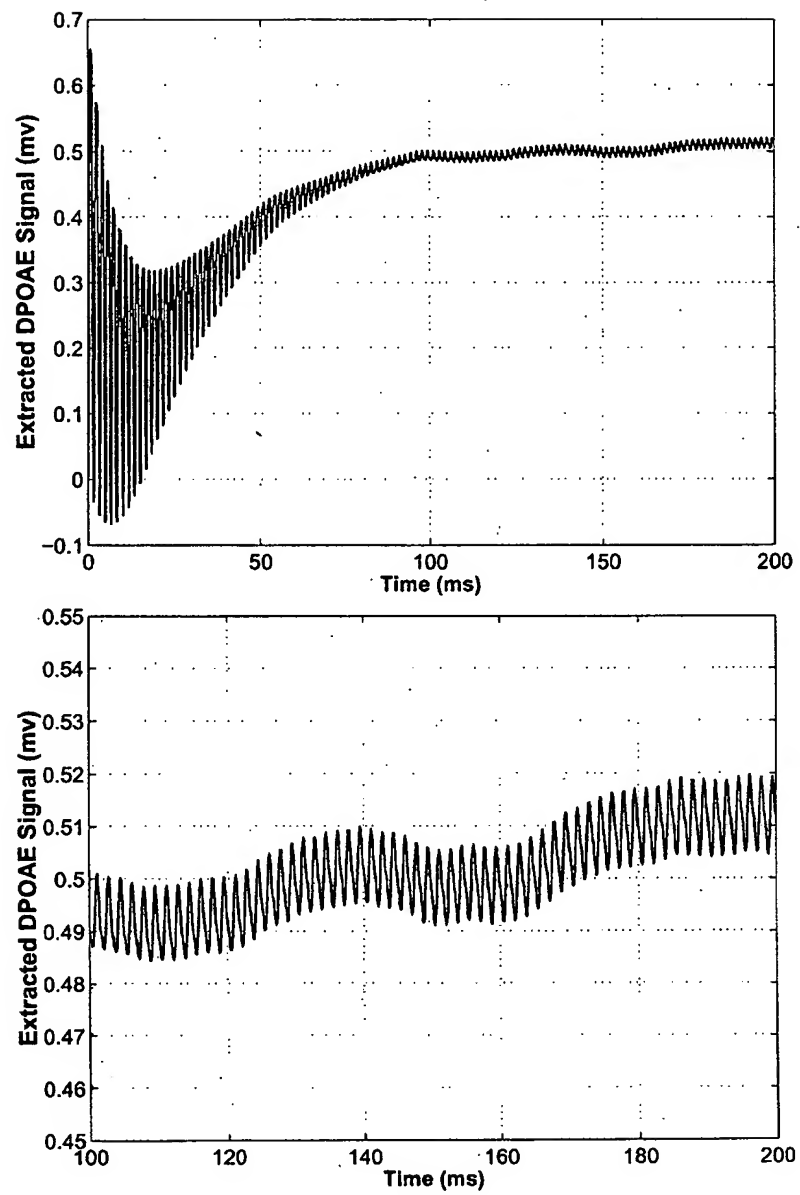
Figure 13: Performance of the present method in estimation of DPOAE in a highly noisy background (SNR=0 dB). The bottom figure is a magnified portion of the top figure.
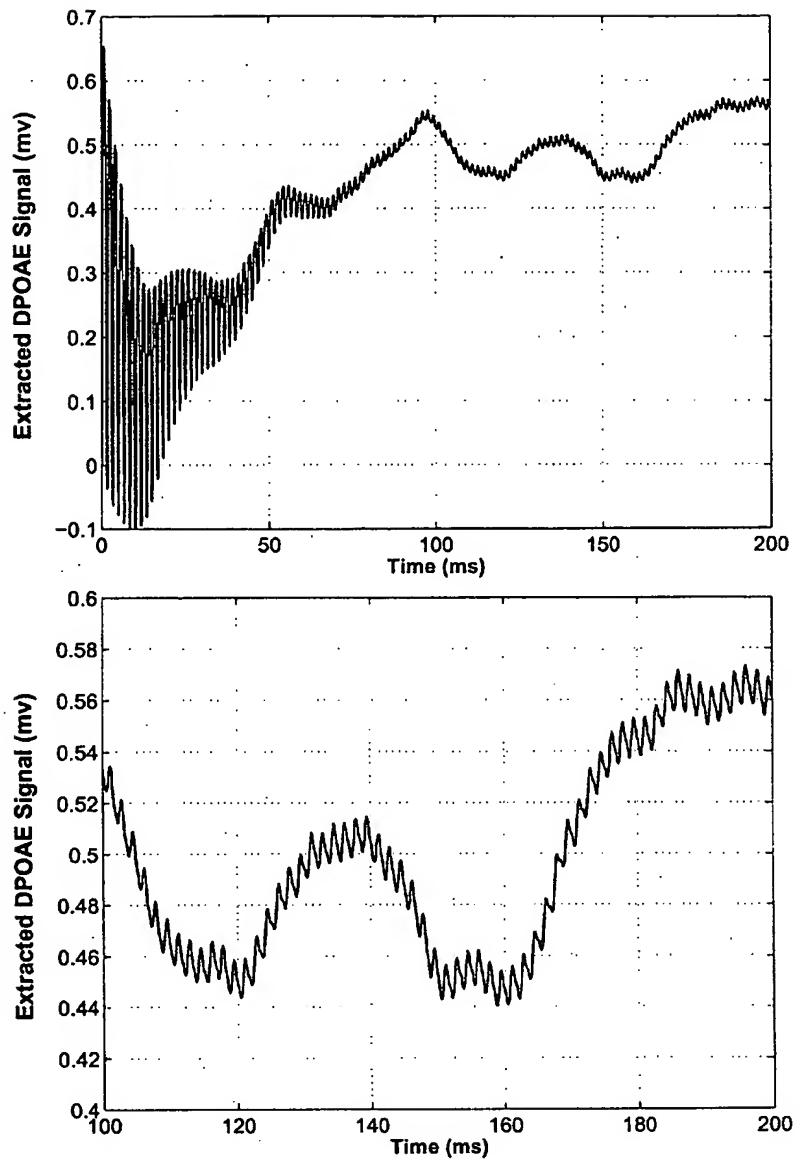
Figure 14: Performance of the present method in estimation of DPOAE in an extremely noisy background (SNR=−20 dB). The bottom figure is a magnified portion of the top figure.

12